AGU PUBLICATIONS

Geophysical Research Letters

RESEARCH LETTER
10.1002/2016GL068935

Key Points:
- Streamflow peaks are likely to decrease for warm regions but increase for cold regions with warming
- Regions susceptible to snow-to-rain transitions are expected to experience distinct decreases in streamflow peaks
- Changes in streamflow peaks with warming are strongly influenced by site-specific meteorological characteristics

Supporting Information:
- Supporting Information S1

Correspondence to:
M. Kumar,
mukesh.kumar@duke.edu

Citation:
Wang, R., M. Kumar, and T. E. Link (2016), Potential trends in snowmelt-generated peak streamflows in a warming climate, *Geophys. Res. Lett.*, *43*, doi:10.1002/2016GL068935.

Received 21 OCT 2015
Accepted 3 MAY 2016
Accepted article online 5 MAY 2016

Potential trends in snowmelt-generated peak streamflows in a warming climate

Rui Wang[1], Mukesh Kumar[1], and Timothy E. Link[2]

[1]Nicholas School of Environment, Duke University, Durham, North Carolina, USA, [2]College of Natural Resources, Department of Forest, Rangeland, and Fire Sciences, University of Idaho, Moscow, Idaho, USA

Abstract Previously reported impacts of climate warming on streamflow peaks are varied, and the controls on the variations remain unclear. Using physically based linked snowpack and watershed hydrological models, we evaluated the potential changes in seasonal snowmelt-generated streamflow peak (Q_{max}) due to warming in a small semiarid mountain watershed. Results suggest that the trend in Q_{max} with warming is strongly governed by the conversion of precipitation phase, accumulated snow amount prior to the melt season, and snowmelt rate during the ablation period. Under a warming climate, the trend in Q_{max} is expected to be decreasing for relatively warm regions but increasing for cold regions. Climate regimes that are most susceptible to dominant precipitation phase transitions from snow to rain are likely to experience larger decreases in Q_{max} with warming. This study serves as a first step toward assessing the varied impacts on Q_{max} due to warming vis-a-vis the specific catchment hydroclimatology.

1. Introduction

Human and agricultural water use in most of the western United States is heavily dependent on snowmelt-generated streamflows [*Bales et al.*, 2006]. To sustainably manage water resources and develop strategies to adapt to climate changes, it is imperative to understand the impacts of climate warming on streamflow dynamics in these cold regions. In this context, impact of climate changes on timing of snowmelt-generated Q_{max} and amount of snowmelt runoff has been widely studied [*Barnett et al.*, 2005; *Ashfaq et al.*, 2013; *Benedetti*, 2008; *Das et al.*, 2011; *Day*, 2009; *Hidalgo et al.*, 2009; *Rauscher et al.*, 2008; *Shrestha et al.*, 2014; *Stewart et al.*, 2005]. Climate warming may also impact the magnitude of seasonal snowmelt-generated Q_{max} [*Molini et al.*, 2011; *Jefferson et al.*, 2008; *Bouwer et al.*, 2008], an important variable for applications such as reservoir operations, flood plain mapping and risk analyses, contaminant transport, nutrient transport, terrestrial carbon cycling, and aquatic and riparian ecology. In this context, using model results *Shrestha et al.* [2011, 2014] and *Wang et al.* [2010] reported an increase in Q_{max} under a climate warming scenario, while *Stonefelt et al.* [2000] reported a decrease in Q_{max}. Statistical analyses of long-term historical data sets also showed the possibility of both a decreasing [*Chiew et al.*, 2013] and an increasing [*Ng et al.*, 2007] trend in Q_{max} with climate warming. Based on the aforementioned studies, the impact of increasing temperature on the magnitude of Q_{max} appears to vary both in sign and magnitude, and the controls on its variations remain unclear. *Molini et al.* [2011] made significant headway in the understanding of Q_{max} trends and indicated that either increasing or decreasing trends may occur depending on the relative length of cold versus warm seasons. The study was based on a synthetic data set, and assumed that (i) precipitation during the cold and warm seasons are entirely in the form of snow and rain, respectively; (ii) precipitation and melt rates are constant during the cold and warm seasons, respectively; and (iii) the melt rate magnitude is linearly proportional to the warm season length. The existence of aforementioned trends vis-à-vis changes in air temperature and snow-to-rain transition remains to be examined.

This study evaluates the potential trends in Q_{max} with warming air temperatures in a small semiarid mountain catchment. Additionally, it addresses the following four questions: (1) Is there a trend in the variation of snowmelt-generated Q_{max} with increasing air temperatures, and what are the major controls on this trend? (2) How does the volume and temporal distribution of snow and rain events mediate the trend in Q_{max}? (3) How are trends in Q_{max} affected by the seasonality of air temperature? and (4) Are the changes in Q_{max} due to climate warming likely to vary across the western U.S. and can these variations be explained based on site-specific climatological characteristics?

2. Data and Methods

A linked snow model ISNOBAL [*Marks et al*., 1999] and hydrologic model PIHM (Penn State Integrated Hydrologic Model) [*Qu and Duffy*, 2007; *Kumar*, 2009] was used to evaluate the influence of warming temperatures on Q_{max}. ISNOBAL is a two-layer coupled energy and mass balance snow model designed for accumulation and melt simulations over digital elevation model grids. PIHM is a fully distributed hydrologic model designed for spatially explicit simulations of interception, overland flow, soil moisture, evapotranspiration, groundwater, and streamflow at multiple scales [*Chen et al*., 2015; *Kumar and Duffy*, 2015; *Yu et al*., 2014].

The linked model was applied in the Reynolds Mountain East (RME) watershed (Figure S1 in supporting information), a field laboratory in southwestern Idaho. The watershed is 0.39 km^2 in area and ranges in elevation from 2027 m to 2137 m. Approximately 30% of the watershed is forested and the remainder consists of dry meadows and mixed shrub species. The watershed received about 75% of its precipitation in the form of snow during the study period. The site was selected because of its high-quality data [*Reba et al*., 2011] and extensive validation of both ISNOBAL [*Marks and Winstral*, 2001; *Marks et al*., 2002] and PIHM [*Kumar et al*., 2013; *Wang et al*., 2013] in the watershed.

Snowmelt and streamflow in the RME watershed was simulated using a 25 year (1984–2008 water year) hourly data set of precipitation, air temperature, dew point temperature, relative humidity, and wind speed [*Reba et al*., 2011]. Precipitation was classified as snow when the dew point temperature was below 0°C [*Marks et al*., 2013]. Net radiation was calculated using the toporad and trad functionalities in the Image Processing Workbench software [*Image Processing Workbench*, 2016]. Validation of the linked model to effectively simulate annual runoff, annual maximum and hourly streamflow, annual maximum and hourly snow water equivalent (SWE), soil moisture, and groundwater depth is shown in Figures S2, S3, and S4. Notably, the model was able to adequately capture the peak streamflows during the 25 year simulation period, as indicated by root mean square error (RMSE), coefficients of determination (CD), and Nash-Sutcliffe efficiency (NSE) of 0.02 m^3/s, 0.84, and 0.82, respectively (Figure S2).

Four suites of numerical experiments were conducted to address the four questions outlined in section 1. The experiments consisted of a combination of different warming *scenarios* and climate *regimes*, each with three *cases* that represented different warming period during a year. Details of each experiment is as follows:

1. To evaluate the trends in Q_{max} with warming, Experiment 1 employed five scenarios with different mean air temperatures. The temperature series for each of the five scenarios were obtained by adding ΔT (ranging from 0 to +4°C in 1°C increments) to the base meteorological data series, to assess the full range of temperature increases that are projected within the next century [*New et al*., 2011]. To explore the relative role of snow accumulation and melt season on Q_{max} trends, ΔT was applied in the entire year (Case 1), only in the cold season (Case 2) and only in the warm season (Case 3). The cold and warm seasons were defined as the period from October–March and April–September, respectively. Specifications of the five warming scenarios and the three seasonality cases are shown in Table S1 (see supporting information).
2. To explore the role of snow and rain events on the Q_{max} trends, Experiment 2 consisted of a base climatological time series and two additional meteorological regimes with different volumes and temporal distribution of snow and rain events. For each regime, five warming scenarios and three cases, identical to the ones used in Experiment 1, were considered. Precipitation events were reordered during the cold season to produce two distinct time series such that the magnitude of snow-to-rain transition (STRT) volumes with increasing temperatures would be different relative to the base configuration. While all the three regimes had 25% of the annual precipitation in form of rain for the initial temperature series, ratios of precipitation in the temperature range ($T < -4$°C) and ($-4°C \leq T < 0°C$) for the three regimes were 32:43, 65:10, and 10:65, respectively. As such, the first/third regime was expected to experience the smallest/largest STRT with ΔT increasing from 0 to +4°C. The three STRT regimes were then repeated for three additional rescaled precipitation series with magnitudes equal to 50%, 150%, and 200% of the base set cases. In all, Experiment 2 involved a total of 180 25 year hydrologic simulations (three rain/snow distribution × four precipitation magnitude = 12 regimes, with each having five warming scenarios and three cases, see Table S2).
3. Experiment 3 also considered five warming scenarios and three cases, with ΔT being identical to those used in Experiments 1 and 2. These scenarios were implemented for 36 (6 × 6) different climatological regimes representing either warmer or colder cold and warm seasons relative to the base temperature series. The 6 × 6 gradually warming cold/warm season regimes were generated by keeping temperatures

Table 1. Average Annual Precipitaton (P), Cold Season Temperature (T_c), Warm Season Temperature (T_w), Snow-to-Rain Conversion Rate (ΔS), Absolute Variation in $Q_{max,v}$ ($\Delta Q_{max,a}$) and Relative Variation in $Q_{max,v}$ ($\Delta Q_{max,r}$) With 2°C Increases in air Temperatures for RME and 11 SNOTEL Sites in Experiment 4[a]

Site Name	State	Latitude	Longitude	Elevation (m)	P (mm)	T_c (°C)	T_w (°C)	ΔS (%)	$\Delta Q_{max,a}$ (mm)	$\Delta Q_{max,r}$ (%)	Simulation Period
RME	ID	43.3	−116.6	2059	966	−1.1	10.4	−30	−0.30	−23.8	1984–2008
Fry	AZ	35.1	−111.8	2195	678	1.9	14	−29	−0.11	−20.0	1984–2014
Virginia Lakes Ridge	CA	38.1	−119.2	2879	670	−1.1	8.9	−18	−0.17	−19.8	1992–2014
Ivanhoe	CO	39.3	−106.6	3170	893	−5.2	7.7	−9	0.04	4.4	1992–2014
Niwot	CO	40	−105.5	3021	820	−3.5	7.5	−11	−0.14	−13.0	1990–2014
Tower	CO	40.5	−106.7	3200	1480	−6.5	6.6	−5	0.16	7.8	1986–2014
Banner Summit	ID	44.3	−115.2	2146	1030	−3.6	8.7	−22	−0.19	−13.9	1989–2014
Sylvan Lake	WY	44.5	−110.2	2566	975	−6.1	6.8	−3	0.12	8.2	1984–2014
West Yellowstone	MT	44.7	−111.1	2042	608	−3.8	10.0	−9	−0.07	−8.9	1999–2014
Touchet	WA	46.1	−117.8	1685	1380	−0.1	10.7	−42	−0.38	−23.2	1984–2014
Stampede Pass	WA	47.3	−121.3	1173	2240	−0.7	8.6	−40	−0.45	−20.1	1984–2014
Poorman Creek	MT	48.1	−115.6	1555	1900	−1.3	10.0	−46	−0.41	−22.7	1999–2014

[a]Here ΔS is considered as the percentage of relative change in snowfall amount with 2°C increases in air temperatures. Simulation period for each site was determined by data availability.

in one of the seasons unchanged at their base level while altering the temperatures in the other season by −6 to 4°C in 2°C steps with respect to the base level. In all, Experiment 3 involved a total of 540 ($6 \times 6 = 36$ temperature regimes, with each having five warming scenarios and three temperature change cases, see Table S3) 25 year simulations with average cold and warm season temperatures ranging from −7 to +3°C and +5 to +15°C, respectively. Although some of the cold/warm season temperature combinations were outside the realm of conditions that would be reasonably expected in the western U.S., they were included for completeness of the sensitivity study and are indicated by the gray shaded figures shown in Figure 3.

4. To evaluate if the derived trends in Q_{max} obtained by modulating meteorological data at RME in Experiment 3 may indeed occur at other sites, and if the differences in these trends can be explained by site's climatology, Experiment 4 involved performing hydrologic simulations on a virtual watershed with same properties as that of RME but using hydrometeorological data from 11 Snow Telemetry (SNOTEL) sites ranging from 35 to 48°N and 105 to 121°W in the western U.S. (Table 1). Use of the virtual watershed enables isolation of climate regimes from watershed-based controls on the Q_{max} trends. The simulations are not intended to be representative of the specific locations as the sites differ in their ecological, physiographic, and hydrogeologic characteristics but are used to test the sensitivity of different climate regimes to warming using observed meteorological data. Meteorological data for the 11 test sites were obtained from SNOTEL (SNOTEL, 2016, http://www.wcc.nrcs.usda.gov/snow/snotel-data.html) and National Climatic Data Center (NCDC) (NCDC, 2016, https://www.ncdc.noaa.gov/data-access) databases. Since long-term hourly records are not available at SNOTEL sites, hourly precipitation, air temperature, and dew point temperature for these sites were obtained from the nearest NCDC sites with similar elevations. Validation of simulation results showed that the model was able to capture the variations in annual maximum SWE across all the 11 sites (Figure S5).

3. Results and Discussion

Results from the four numerical experiments are presented thematically following the four questions outlined in section 1.

3.1. Is There a Trend in Snowmelt-Generated Q_{max}, and What Are the Major Controls on This Trend?

Figure 1 shows the trends in Q_{max} for the three warming cases in Experiment 1. As the temperature during the entire year increases from Scenarios 1 to 5 ($\Delta T = 0$ to +4°C), the 25 year average Q_{max} decreased from 0.13 to 0.07 m^3/s (~46% reduction, Figure 1d). The variations in average Q_{max} can be explained based on five scenario simulations with increasing ΔT applied separately in the cold and warm seasons. As temperatures during the cold season increased from Scenarios 1 to 5 ($\Delta T_c = 0$ to +4°C), the 25 year average $Q_{max,\Delta Tc}$ decreased from 0.13 to 0.06 m^3/s (Figure 1e). This is because warmer cold seasons result in a smaller fraction of precipitation in the form of snowfall, which in turn leads to a smaller snow accumulation and $Q_{max,\Delta Tc}$ (Figure S6, Case 2). As temperatures during the warm season increased from Scenarios 1 to 5 ($\Delta T_w = 0$ to +4°C), the 25 year average $Q_{max,\Delta Tw}$

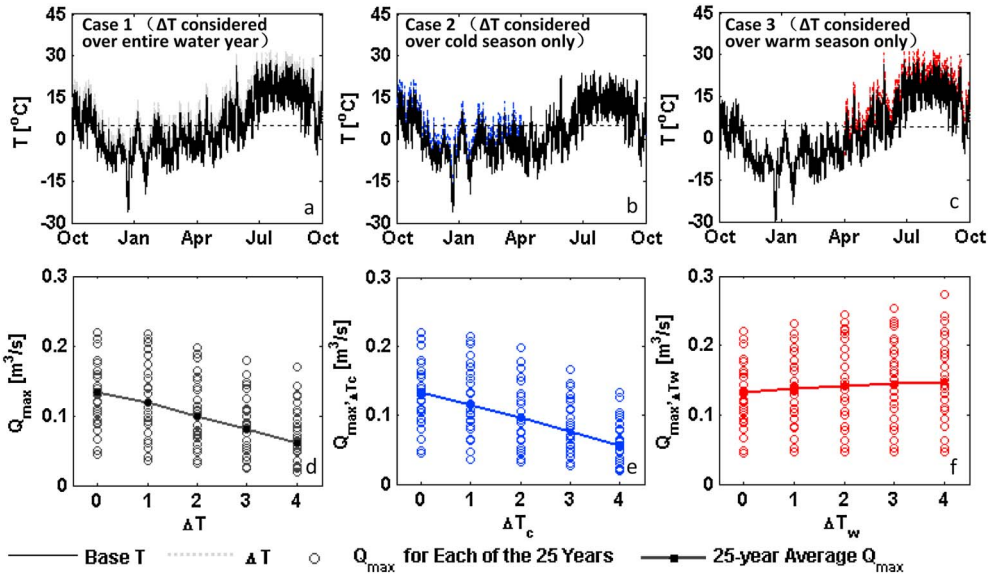

Figure 1. Q_{max}, $Q_{max,\Delta Tc}$/$Q_{max,\Delta Tw}$ for scenarios with $\Delta T/\Delta T_c/\Delta T_w$ ranging from 0 to +4°C from Scenarios 1 to 5. For visual clarity, Figures 2a–2c only show temperature series for the 1984 water year. ΔT, ΔT_c, and ΔT_w indicate the increase in temperatures during the entire year, warm, and cold seasons, respectively. Q_{max}, $Q_{max,\Delta Tc}$, and $Q_{max,\Delta Tw}$ refer to simulated streamflow peak with temperature being equal to base temperature plus ΔT, ΔT_c, and ΔT_w, respectively. The rates of increase/decrease in Q_{max}, $Q_{max,\Delta Tc}$, and $Q_{max,\Delta Tw}$ from Scenarios 1 to 5 are listed in Table S1 in the supporting information.

increased slightly due to increase in late season melt rates (Figure 1f). This is because increases in temperatures during the warm season increases the melt rate due to increased sensible heat and longwave radiation to the snow pack, thus increasing discharge per accumulated snow amount (Figure S6, Case 3). The relative influence of these two competing controls ends up determining the trend in Q_{max}. As the decrease in $Q_{max,\Delta Tc}$ was larger than the increase in $Q_{max,\Delta Tw}$ for RME, Q_{max} showed a decreasing trend.

3.2. How Does the Volume and Temporal Distribution of Snow and Rain Events Mediate the Trend in Q_{max}?

Results from Experiment 2 indicate that in regimes with small STRT, Q_{max} showed a very slightly increasing trend with temperature. In contrast, with increasing STRT amounts, Q_{max} showed a tendency for a decreasing trend (Figure 2). Variations in the trends are again explainable based on competition between the slope of $Q_{max,\Delta Tw}$ and $Q_{max,\Delta Tc}$. Consistent with the findings in section 3.1, as ΔT_w increased from Scenarios 1 to 5, $Q_{max,\Delta Tw}$ increased due to increasing late season melt rates (Figures 2d, 2h, and 2l). Also, $Q_{max,\Delta Tc}$ decreased with increase in ΔT_c due to lower snow accumulations (Figures 2c, 2g, and 2k). The decrease in $Q_{max,\Delta Tc}$ was smaller/larger for the case with small/large STRT. As a result, Q_{max} showed an increasing trend for the small STRT regime and a decreasing trend for the large STRT regime (Figures 2b, 2f, and 2j). In addition, Figure 2 highlights that the simulated variations in Q_{max} were also a function of precipitation magnitude. For example, increase in $Q_{max,\Delta Tw}$ between Scenarios 1 to 5 was generally larger for higher annual precipitation magnitudes, because $Q_{max,\Delta Tw}$ in this case was not limited by the amount of snow available for melt (e.g., Figure 2h). Decrease in $Q_{max,\Delta Tc}$ between Scenarios 1 to 5 was also larger for higher annual precipitation magnitudes due to greater decreases in snow amount with warming (e.g., Figure 2g). Based on the relative magnitude of variations in $Q_{max,\Delta Tw}$ and $Q_{max,\Delta Tc}$, the trend in Q_{max} was generally more obvious with increasing magnitude of annual precipitation (Figure 2f).

3.3. How is the Trend in Q_{max} Affected by the Seasonality of Air Temperature?

Results from Experiment 3 show four notable variations (Figure 3):

1. As average temperature during the warm season (T_w) increased from +5 to +15°C, Q_{max} for a given warming scenario also increased. This was mainly because higher T_w, i.e., warmer melt season increased melt rates, leading to an increase in Q_{max}. For climate regimes with relatively high temperatures in warm or

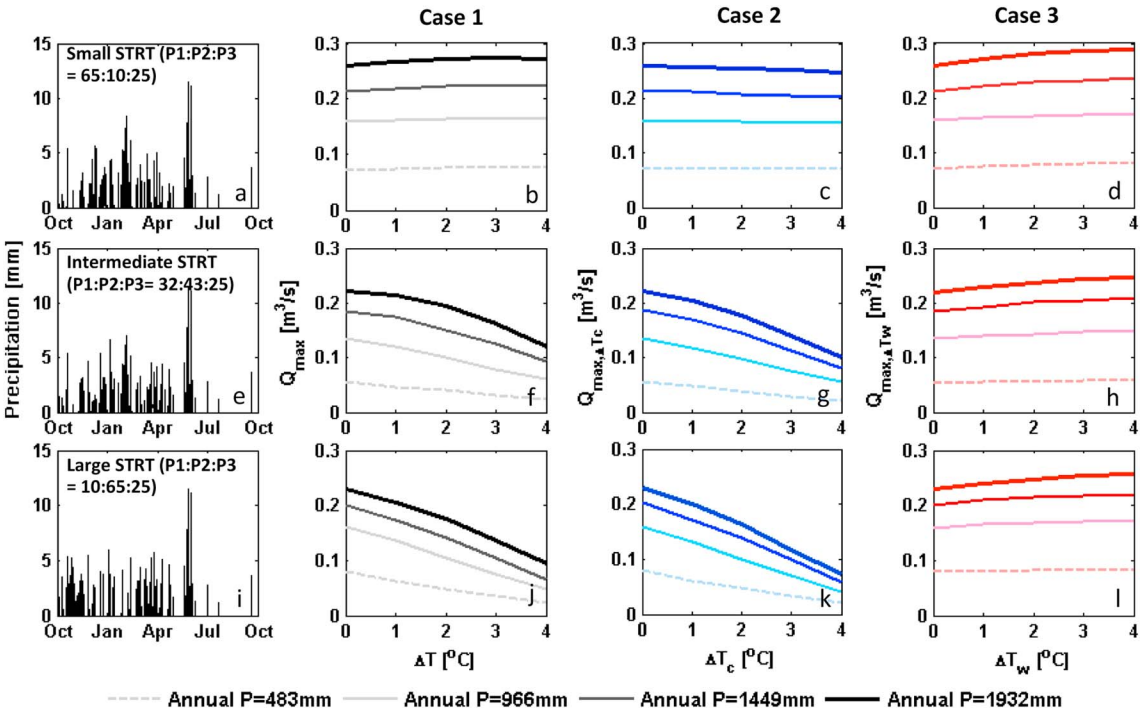

Figure 2. Variation in 25 year average Q_{max}, $Q_{max,\Delta Tc}$, and $Q_{max,\Delta Tw}$ from Scenarios 1 to 5 for $\Delta T/\Delta T_c/\Delta T_w$ ranging from 0 to +4°C for precipitation regimes with different magnitude of snow-to-rain transition (STRT) and mean annual precipitation. P1, P2, and P3 refer to the percent of precipitation occurring when $T < -4$°C, -4°C $\leq T < 0$°C, and $T \geq 0$°C, respectively. The rate of increase/decrease in Q_{max}, $Q_{max,\Delta Tc}$, and $Q_{max,\Delta Tw}$ are, respectively, listed in Tables S2-1, S2-2, and S2-3 in the supporting information.

cold seasons (e.g., $T_w = 15$°C and $T_c = 3$°C), increase in $Q_{max,\Delta Tw}$ with increasing T_w was miniscule because melt was mass, rather than energy limited.

2. As average temperature during the cold season (T_c) increased from -7.0 to 3.0°C, Q_{max} for a given scenario decreased. This was mainly because the snow accumulation amount at the end of warmer cold seasons (higher T_c) was much smaller.
3. The variation in Q_{max} with increase in temperature showed a tendency toward decreasing trends for relatively warmer warm seasons. For example, for T_c equal to -5°C in Figure 3, Q_{max} showed an increasing trend for very cold warm seasons (e.g., $T_w = 5$°C), an increasing followed by a decreasing trend for intermediate cases (e.g., $T_w = 9$°C) and a decreasing trend for warmer warm seasons (e.g., $T_w = 15$°C). To explain the trends, we analyzed the variations in $Q_{max,\Delta Tc}$ and $Q_{max,\Delta Tw}$ with increasing T_w in isolation: (a) The rate of decrease in $Q_{max,\Delta Tc}$ from Scenarios 1 to 5 increased as T_w increased from +5 to +15°C (Figure 3). This was because of larger/smaller increase in $Q_{max,\Delta Tc}$ with T_w for lower/higher ΔT_c scenario (Figure 3). For scenarios with lower ΔT_c, snow volume was larger and Q_{max} increased with increasing T_w due to higher melt rates (Figure S7). In contrast, for scenarios with higher ΔT_c, snow volume was smaller and hence the peak melt was mass, rather than energy limited (Figure S7). This leads to a subdued rate of increase in $Q_{max,\Delta Tc}$ with increasing T_w. (b) The rate of increase in $Q_{max,\Delta Tw}$ from Scenarios 1 to 5 became smaller as T_w increased from +5 to +15°C (Figure 3). This was mainly because for large T_w, melt for both low and high ΔT_w scenarios were limited by snow amount available for melt, thus limiting the increase in Q_{max} from Scenarios 1 to 5 (Figure S8). Hence, warmer warm seasons reduce the positive slope of $Q_{max,\Delta Tw}$ and strengthen the negative slope of $Q_{max,\Delta Tc}$, thus pushing Q_{max} variations toward a decreasing trend.
4. The variation of Q_{max} with increases in temperature showed a tendency toward decreasing trends for relatively warmer cold seasons. For example, for $T_w = 9$°C in Figure 3, Q_{max} showed an increasing trend with warming for very cold cold seasons (e.g., $T_c = -7$°C), an increasing followed by a decreasing trend for intermediate temperatures (e.g., $T_c = -5$°C) and a decreasing trend for warmer cold seasons (e.g., $T_c = 1$°C). This is because precipitation was generally in the form of snow during colder winters, thus resulting in larger snow accumulation volumes. This leads to a larger slope of increasing $Q_{max,\Delta Tw}$. In contrast, the rate of decrease in $Q_{max,\Delta Tc}$ was smaller in very cold winters due to the smaller likelihood of STRT with increasing

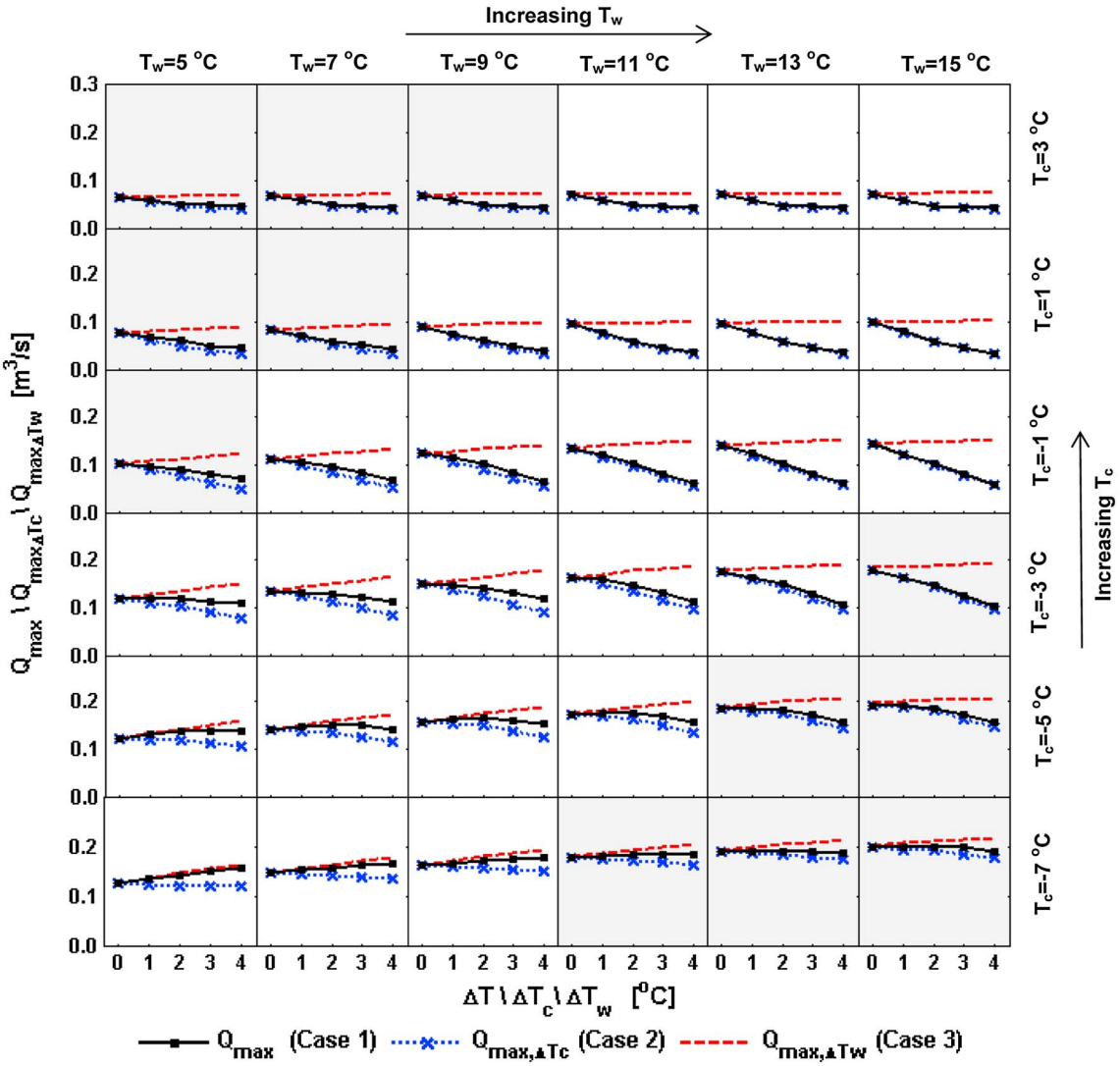

Figure 3. Variation in 25 year average Q_{max}, $Q_{max,\Delta Tc}$, and $Q_{max,\Delta Tw}$ from Scenarios 1 to 5 for $\Delta T/\Delta T_c/\Delta T_w$ ranging from 0 to +4°C for temperature regimes with either warmer or colder cold and warm seasons. T_c and T_w refers to average cold and warm season temperature, respectively. Shaded plots represent temperature combinations that are outside the range of typical western U.S. locations but are provided for completeness. The rate of increase/decrease in Q_{max}, $Q_{max,\Delta Tc}$, and $Q_{max,\Delta Tw}$ from Scenarios 1 to 5 are, respectively, listed in Tables S3-1, S3-2, and S3-3 in the supporting information.

temperatures. Hence, colder winter regimes dampen the negative slope of $Q_{max,\Delta Tc}$ and enhance the positive slope of $Q_{max,\Delta Tw}$, thus pushing Q_{max} toward increasing trends with warmer temperatures.

The last two highlighted variations also show that for cold climate regimes where the mean temperatures are relatively low during the entire year (e.g., $T_w = 5$°C and $T_c = -7$°C), changes in Q_{max} with warming is expected to be increasing, while for warmer climate regimes with higher mean temperatures (e.g., $T_w = 15$°C and $T_c = 3$°C), changes in Q_{max} with warming is expected to be decreasing.

3.4. Are the Changes in Q_{max} Due to Climate Warming Likely to Vary Across the Western U.S., and can These Variations be Explained Based on Site-Specific Climatological Characteristics?

Experiment 4 evaluated variations in Q_{max} over the virtual watershed (henceforth referred as $Q_{max,v}$) for a 2°C increase in air temperature at 11 SNOTEL sites (Table 1). The 2°C increase in air temperature was selected as an approximation of predicted changes 50 years into the future [*New et al.*, 2011]. Change in $Q_{max,v}$ was positive for three sites and negative for the other nine sites. While the sites covered a wide range of hydroclimatic conditions, the snow-to-rain transition rates, annual precipitation, and temporal distribution of rain versus

snow events, the variation in trends across the sites appears to be in general agreement with the trends presented in the previous sections. For example, $Q_{max,v}$ at Stampede Pass, Touchet, and Poorman Creek experienced relatively large decreases in $Q_{max,v}$ with a 2°C warming because of the relatively warmer winters and higher STRT rates with increasing temperatures. In contrast, $Q_{max,v}$ at Ivanhoe, Tower, and Sylvan Lakes increased with warming due to very cold winter conditions and relatively small rates of STRT. Although the rate of STRT was relatively small for the West Yellowstone site too, $Q_{max,v}$ still showed a decreasing trend. This is because of the relatively low annual precipitation that mainly occurs as snow at this location, leading to relatively low total accumulations. As a result, potential increase in flow rates with warming is mass, rather than energy limited at the site. Annual precipitation at Banner Summit is similar to the annual precipitation at Sylvan Lake, but $Q_{max,v}$ at Banner Summit exhibited a decreasing trend due to relatively warmer winter conditions and larger ratio of STRT. Results suggest that the trend in Q_{max} with warming is strongly determined by site-specific hydrometerological characteristics.

4. Conclusions

The study reports the potential variations in snowmelt-generated peak streamflows (Q_{max}) in response to a warmer climate, for a wide range of temperature and precipitation regimes. The results show that the trend in Q_{max} in the RME watershed is expected to be decreasing as the climate warms. Furthermore, for altered climatological configurations, the trend in Q_{max} may become monotonically increasing, monotonically decreasing, or increasing followed by a decreasing trend. Also, the trend is likely to be increasing/decreasing for regions with relatively warm/cold temperatures. Aforementioned variations in Q_{max} trends are a result of interactions between reduced snow accumulations and increased late season melt rates with warming temperatures. Notably, the relative influence of these two competing factors are found to be strongly influenced by the seasonal variations of temperatures, precipitation magnitudes, the ratio of snow:rain events, and the temporal distribution of snow and rain events. Regions susceptible to snow-to-rain transitions are expected to experience distinct decreases in Q_{max} due to warming. The changes in Q_{max} due to warming are likely to vary across the western U.S. with variations being strongly influenced by the site-specific meteorological characteristics.

It should be emphasized that this study focused on trends in long-term averaged Q_{max} generated by seasonal snowmelt processes in a small watershed. Watershed characteristics such as topography [*Tennant et al*., 2015a], scale [*Tennant et al*., 2015b], vegetation, and hydrogeology [*Harder et al*., 2015] may affect the specific trends noted in this research. As such, evaluating changes to peakflow generating processes across a range of scales, geologies, and hydroclimates will also be important to develop a comprehensive understanding of how climate changes may affect streamflow regimes. Despite these limitations, the results underscore the occurrence of varied trends in Q_{max} with climate warming based on site's meteorological characteristics and highlight the need for site-based analyses to guide the development of water resource and ecosystem adaptation strategies to reduce the impacts of changing climate on Q_{max} regimes.

Acknowledgments
This study was supported by the Duke University start-up grant and NSF CAREER award (EAR 1454983). Preparation of this publication was also supported by the DOI NWCSC through a Cooperative Agreement GS296A-A from the United States Geological Survey (USGS). Its contents are solely the responsibility of the authors and do not necessarily represent the views of funding organizations. The RME data presented in this article were generated by Northwest Watershed Research Center, USDA, and distributed by ftp://ftp.nwrc.ars.usda.gov/public/RME_25yr_database. We thank Editor Bayani Cardenas and two anonymous reviewers for constructive comments that greatly improved this paper.

References

Ashfaq, M., S. Ghosh, S.-C. Kao, L. C. Bowling, P. Mote, D. Touma, S. A. Rauscher, and N. S. Diffenbaugh (2013), Near-term acceleration of hydroclimatic change in the western U.S., *J. Geophys. Res. Atmos.*, *118*, 10,676–10,693, doi:10.1002/jgrd.50816.

Bales, R. C., N. P. Molotch, T. H. Painter, M. D. Dettinger, R. Rice, and J. Dozier (2006), Mountain hydrology of the western United States, *Water Resour. Res.*, *42*, W08432, doi:10.1029/2005WR004387.

Barnett, T. P., J. C. Adam, and D. P. Lettenmaier (2005), Potential impacts of a warming climate on water availability in snow-dominated regions, *Nature*, *438*, 303–309, doi:10.1038/nature04141.

Benedetti, M. M. (2008), Future changes in snowmelt-driven runoff timing over the western US, *Geophys. Res. Lett.*, *35*, L16703, doi:10.1029/2008GL034424.

Bouwer, L. M., J. E. Vermaat, and J. C. J. H. Aerts (2008), Regional sensitivities of mean and peak river discharge to climate variability in Europe, *J. Geophys. Res.*, *113*, D19103, doi:10.1029/2008JD010301.

Chen, X., M. Kumar, and B. L. McGlynn (2015), Variations in streamflow response to large hurricane-season storms in a southeastern US watershed, *J. Hydrometeorol.*, *16*(1), 55–69, doi:10.1175/JHM-D-14-0044.1.

Chiew, S. Y., O. S. Selaman, and N. R. Afshar (2013), A study on the relationship between climate change and peak discharge in Sarawak River Basin, *UNIMAS e-J. Civ. Eng.*, *4*(3), 23–28.

Das, T., D. W. Pierce, D. R. Cayan, J. A. Vano, and D. P. Lettenmaier (2011), The importance of warm season warming to western U.S. streamflow changes, *Geophys. Res. Lett.*, *38*, L23403, doi:10.1029/2011GL049660.

Day, C. A. (2009), Modelling impacts of climate change on snowmelt runoff generation and streamflow across western US mountain basins: A review of techniques and applications for water resource management, *Prog. Phys. Geogr.*, *33*, 614–633, doi:10.1177/0309133309343131.

Harder, P., J. W. Pomeroy, and C. J. Westbrook (2015), Hydrological resilience of a Canadian Rockies headwaters basin subject to changing climate, extreme weather, and forest management, *Hydrol. Processes*, *29*(18), 3905–3924, doi:10.1002/hyp.10596.

Hidalgo, H. G., et al. (2009), Detection and attribution of streamflow timing changes to climate change in the western United States, *J. Clim.*, *22*(13), 3838–3855, doi:10.1175/2009JCLI2470.1.
Image Processing Workbench (2016), Image processing workbench. [Available at http://cgiss.boisestate.edu/~hpm/software/IPW/installV2.html, Accessed on Feb 17, 2016.]
Jefferson, A., A. Nolin, S. Lewis, and C. Tague (2008), Hydrogeologic controls on streamflow sensitivity to climate variation, *Hydrol. Processes*, *22*(22), 4371–4385, doi:10.1002/hyp.7041.
Kumar, M. (2009), Toward a Hydrologic Modeling System, PhD dissertation, Civ. and Environ. Eng., Pa. State Univ. [Available at https://etda.libraries.psu.edu/paper/9870/5576.]
Kumar, M., and C. J. Duffy (2015), Exploring the role of domain partitioning on efficiency of parallel distributed hydrologic model simulations, *J. Hydrogeol. Hydrol. Eng.*, *4*, 1, doi:10.4172/2325-9647.1000119.
Kumar, M., D. Marks, J. Dozier, M. Reba, and A. Winstral (2013), Evaluation of distributed hydrologic impacts of temperature-index and energy-based snow models, *Adv. Water Resour.*, *56*, 77–89, doi:10.1016/j.advwatres.2013.03.006.
Marks, D., and A. Winstral (2001), Comparison of snow deposition, the snow cover energy balance, and snowmelt at two sites in a Semiarid Mountain Basin, *J. Hydrometeorol.*, *2*, 213–227, doi:10.1175/1525-7541(2001)002<0213:COSDTS>2.0.CO;2.
Marks, D., J. Domingo, D. Susong, T. Link, and D. Garen (1999), A spatially distributed energy balance snowmelt model for application in mountainous basins, *Hydrol. Processes*, *13*, 1935–1959, doi:10.1002/(SICI)1099-1085(199909)13:12/13<1935::AID-HYP868>3.0.CO;2-C.
Marks, D., A. Winstral, and M. Seyfried (2002), Simulation of terrain and forest shelter effects on patterns of snow deposition, snowmelt and runoff over a semi-arid mountain catchment, *Hydrol. Processes*, *16*, 3605–3626, doi:10.1002/hyp.1237.
Marks, D., A. Winstral, M. Reba, J. Pomeroy, and M. Kumar (2013), An evaluation of methods for determining during-storm precipitation phase and the rain/snow transition elevation at the surface in a mountain basin, *Adv. Water Resour.*, *55*, 98–110, doi:10.1016/j.advwatres.2012.11.012.
Molini, A., G. G. Katul, and A. Porporato (2011), Maximum discharge from snowmelt in a changing climate, *Geophys. Res. Lett.*, *38*, L05402, doi:10.1029/2010GL046477.
New, M., D. Liverman, H. Schroders, and K. Anderson (2011), Four degrees and beyond: The potential for a global temperature increase of four degrees and its implications, *Philos. Trans. R. Soc. A*, *369*, 6–19, doi:10.1098/rsta.2010.0303.
Ng, F., S. Liu, B. Mavlyudov, and Y. Wang (2007), Climatic control on the peak discharge of glacier outburst floods, *Geophys. Res. Lett.*, *34*, L21503, doi:10.1029/2007GL031426.
Qu, Y., and C. J. Duffy (2007), A semidiscrete finite volume formulation for multi-process watershed simulation, *Water Resour. Res.*, *43*, W08419, doi:10.1029/2006WR005752.
Rauscher, S. A., J. S. Pal, N. S. Diffenbaugh, and M. M. Benedetti (2008), Future changes in snowmelt-driven runoff timing over the western US, *Geophys. Res. Lett.*, *35*, L16703, doi:10.1029/2008GL034424.
Reba, M. L., D. Marks, A. Winstral, M. Kumar, and G. Flerchinger (2011), A long-term data set for hydrologic modeling in a snow-dominated mountain catchment, *Water Resour. Res.*, *47*, W07702, doi:10.1029/2010WR010030.
Shrestha, R. R., Y. B. Dibike, and T. D. Prowse (2011), Modelling of climate-induced hydrologic changes in the Lake Winnipeg watershed, *J. Great Lakes Res.*, *38*, 83–94, doi:10.1016/j.jglr.2011.02.004.
Shrestha, R. R., M. A. Schnorbus, A. T. Werner, and F. W. Zwiers (2014), Evaluating hydroclimatic change signals from statistically and dynamically downscaled GCMs and hydrologic models, *J. Hydrometeorol.*, *15*, 844–860, doi:10.1175/JHM-D-13-030.1.
Stewart, I., D. Cayan, and M. Dettinger (2005), Changes toward earlier streamflow timing across western North America, *J. Clim.*, *18*, 1136–1155, doi:10.1175/JCLI3321.1.
Stonefelt, M., T. Fontaine, and R. Hotchkiss (2000), Impacts of climate change on water yield in the Upper Wind River Basin, *J. Am. Water Resour. Assoc.*, *36*, 321–336, doi:10.1111/j.1752-1688.2000.tb04271.x.
Tennant, C. J., B. T. Crosby, S. E. Godsey, R. W. VanKirk, and D. R. Derryberry (2015a), A simple framework for assessing the sensitivity of mountain watersheds to warming-driven snowpack loss, *Geophys. Res. Lett.*, *42*, 2814–2822, doi:10.1002/2015GL063413.
Tennant, C. J., B. T. Crosby, and S. E. Godsey (2015b), Elevation-dependent responses of streamflow to climate warming, *Hydrol. Processes*, *29*, 991–1001, doi:10.1002/hyp.10203.
Wang, J., H. Li, and X. Hao (2010), Responses of snowmelt runoff to climatic change in an inland river basin, Northwestern China, over the past 50 years, *Hydrol. Earth Syst. Sci.*, *14*, 1979–1987, doi:10.5194/hess-14-1979-2010.
Wang, R., M. Kumar, and D. Marks (2013), Anomalous trend in soil evaporation in a semi-arid, snow-dominated watershed, *Adv. Water Resour.*, *57*, 32–40, doi:10.1016/j.advwatres.2013.03.004.
Yu, X., C. Duffy, D. C. Baldwin, and H. Lin (2014), The role of macropores and multi-resolution soil survey datasets for distributed surface–subsurface flow modeling, *J. Hydrol.*, *516*, 97–106.